

## Heat-Cleaned Nextel in MMOD Shielding

Eric L. Christiansen<sup>(1)</sup> and B. Alan Davis<sup>(2)</sup>

<sup>(1)</sup> NASA Johnson Space Center, Mail Code XI5, Houston, TX 77058, USA, Eric.L.Christiansen@nasa.gov

<sup>(2)</sup> Jacobs Engineering Group, NASA Johnson Space Center, Mail Code XI5, Houston, TX 77058, USA, bruce.davis-1@nasa.gov

### ABSTRACT

Meteoroid and orbital debris (MMOD) shielding can include Nextel™ ceramic cloth in the outer layers of the shielding to enhance MMOD breakup. The Nextel fabric can contain size (or sizing) which aids in manufacture of the fabric. Sizing is a starch, oil or waxy material that is added to the rovings and yarns to protect the fibers from being cut or broken during the fabric manufacturing process and by later handling. For spacecraft applications, sizing is removed by heat-cleaning to reduce/eliminate off-gassing during vacuum operations. After the sizing is removed, the fibers in the woven fabric are prone to breakage during handling which reduces fabric strength. Because heat-cleaned Nextel tends to shed fibers that can be irritating to workers, the usual practice for hypervelocity impact tests is to use Nextel with sizing. The reduced strength of heat-cleaned Nextel does not typically effect the performance of MMOD shields with Nextel used in outer layers of the shield, because the density and areal density of the ceramic fibers in the fabric control MMOD breakup (not fabric strength). This paper provides data demonstrating that hypervelocity impact protection performance is not adversely altered for shields containing heat-cleaned Nextel compared to Nextel with sizing.

### 1 INTRODUCTION

The purpose of this work was to determine by impact test if there is a difference in hypervelocity shielding performance between sized and heat-cleaned Nextel. Nextel ceramic fabric is a trade-mark of the 3M Corporation and is a woven product containing aluminoborosilicate fibers (type 312 and 440 Nextel fabrics). Nextel is a common material found in outer and/or intermediate layers (i.e., the shield's bumper or bumpers) of meteoroid and orbital debris (MMOD) shielding (see Fig. 1). This paper focuses on Whipple-type shielding with a Nextel outer bumper as shown on the left in Fig. 1. In practice, the Nextel in the outer bumper can be incorporated as part of an MMOD-toughened thermal blanket, although the work reported here uses only Nextel as the outer bumper. This type of shielding has application in protecting equipment such as exposed electronic boxes on satellites and space stations from MMOD impacts. The Nextel/Kevlar Stuffed Whipple shield depicted in Fig. 1 is used extensively on the International Space Station (ISS) to protect crew modules [1], and the Flexible Multi-Shock shield is used for protecting inflatable modules and has also been used in satellite protection applications such as the large area telescope instrument on the Fermi Gamma-Ray Space Telescope.

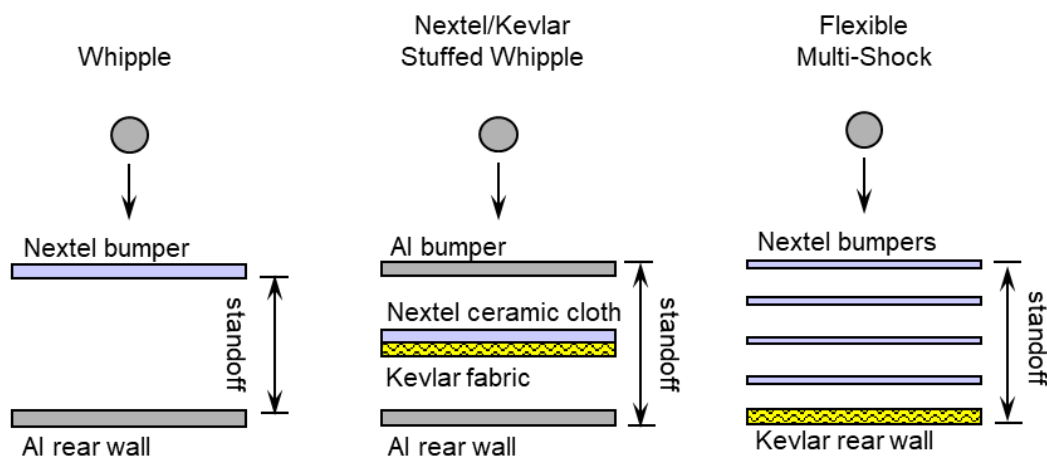


Fig. 1. Three different MMOD shield types using Nextel bumpers.

Nextel ceramic fabric is used in MMOD shields because of certain favorable properties, as listed below.

- (1) Projectile breakup characteristics similar to aluminum. The material density of  $2.8 \text{ g/cm}^3$  for Nextel 312 fiber is comparable to aluminum, and results in shock pressures and projectile breakup comparable to aluminum (Al) bumper materials.
- (2) Low-damage potential from Nextel fragments generated from the fabric during hypervelocity impact. In hypervelocity impact on typical bumper shields such as aluminum plate, fragments from the bumper can result in substantial damage to the rear wall of the shield if the fragments are large enough. However, for Nextel outer bumpers, the fibers that make up the Nextel fabric have diameters between 8 and 14 microns, and typically will break into short lengths during hypervelocity impact. The fragments produced from hypervelocity impact on ceramic fabric will therefore be small and will not create substantial damage to the rear wall of the shield.
- (3) Because it is a flexible fabric, Nextel has the ability to be folded prior to launch and deployed on-orbit as in the case of MMOD shields for inflatable modules. The flexibility provided by Nextel fabric is also important for applications that require conformal or moldable shielding to complex shapes.

The Nextel fabric can contain size (or sizing) which aids in manufacture of the fabric. Sizing is a starch, oil or waxy material that is added to the rovings and yarns to protect the fibers from being cut or broken during the fabric manufacturing process and by later handling. For spacecraft applications, sizing is removed by heat-cleaning to reduce/eliminate off-gassing during vacuum operations. Heat-cleaning is performed by 3M, who accomplishes this process by holding the rolls of fabric in a furnace heated to  $700^\circ\text{C}$  for an unspecified amount of time but likely for several hours [2]. 3M indicates the time required will depend on the furnace design and the amount of material in the furnace. Figure 2 shows magnified images of Nextel 312 style AF10 fabric (used in the study reported here) with sizing and without sizing (after heat-cleaning). Heat-cleaned Nextel has an appearance similar to Nextel with sizing, but with a higher gloss and a few additional broken fibers present.

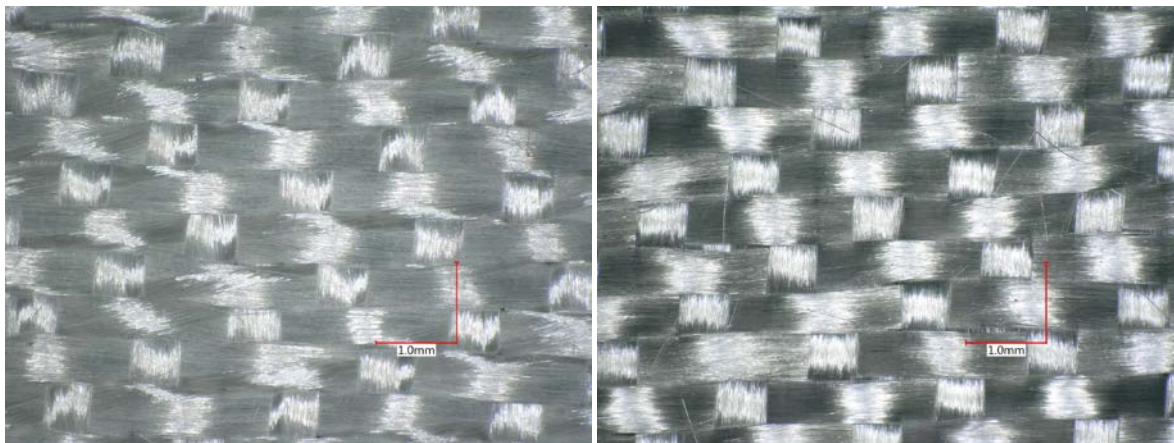


Fig. 2. Nextel 312 style AF10 fabric: with sizing on left and heat-cleaned on right.

3M indicates that heat-cleaning reduces the mass per unit area of Nextel 312 style AF10 fabric by about 17%; i.e., AF10 mass per unit area decreases from  $0.029 \text{ g/cm}^2$  with sizing to  $0.024 \text{ g/cm}^2$  when heat-cleaned [2]. The reduction in areal density results from removal of the sizing, not a reduction in the mass of the ceramic fibers which are unaffected by the temperature used in the heat-cleaning process. Based on just the fiber strength, 3M shows that 100% of the strength of Nextel 312 fiber is retained after 100 hours at  $700^\circ\text{C}$ . After the sizing is removed, the fibers in the woven fabric are prone to breakage during handling which can reduce fabric strength. Fabric breaking strength is typically provided for Nextel 312 fabrics after heat-cleaning. Comparable fabric strength with sizing is not available. While data is limited for fabrics, 3M data indicates that sewing thread made from heat-cleaned Nextel 312 fiber retains 60% of the breaking load of sewing thread made from Nextel 312 fiber with sizing. While data on the breaking strength of the fabric with sizing used in this study is not available, it is believed that the breaking strength of the fabric with sizing is greater, by perhaps 50% or more, compared to the equivalent heat-cleaned fabric based on the thread data. The question this paper addresses is how the lower areal density and strength of heat-

cleaned Nextel affects the hypervelocity ballistic performance of typical MMOD shields compared to Nextel with sizing.

There is another thermal process used to remove sizing, which is referred to as heat-treatment. Heat-treatment is performed at higher temperatures than heat-cleaning, at temperatures of 900°C, and changes the crystalline structure of the Nextel fibers. This paper does not address heat-treated Nextel (only heat-cleaned Nextel).

## 2 HYPERVELOCITY IMPACT TESTS

Hypervelocity impact tests were performed at the NASA White Sands Test Facility (WSTF) on typical Nextel containing shield targets. The 4.3 mm diameter two-stage light-gas launcher at WSTF was used in the testing (Fig. 3) [3].



Fig. 3. WSTF 4.3 mm two-stage light-gas launcher.

### 2.1 Target Description

The configuration of the test articles is shown in Fig. 4. The bumper is composed of 2 layers of Nextel 312 style AF10, either sized or heat-cleaned. Nextel AF10 fabric contains 600 denier yarn in a 46 warp by 46 fill thread count in a 5-harness satin weave type. Nominal thickness is 0.41 mm sized and 0.28 mm heat cleaned. Breaking strength is 25 kg/cm in both warp and fill directions. The total areal density of sized Nextel is 0.058 g/cm<sup>2</sup> and heat-cleaned Nextel is 0.048 g/cm<sup>2</sup>. The rear wall was located 2.5 cm behind the bumper and was 2.0 mm thick Al 6061-T6 aluminum plate. A 1.0 mm thick Al 2024-T3 witness plate was mounted 5.0 cm behind the rear wall to record penetration effects if the rear wall was perforated or exhibited detached spall by the test. The lateral dimensions of each target layer was 30cm wide by 30cm long.

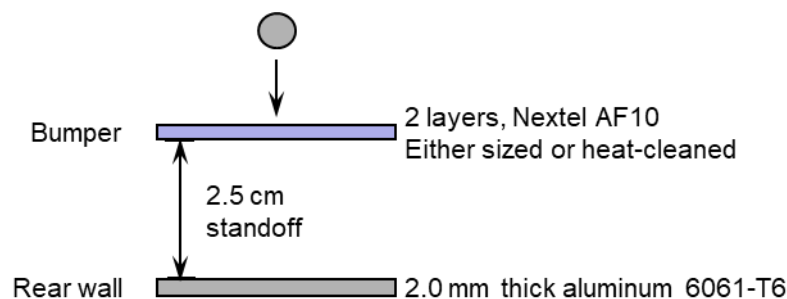


Fig. 4. Target cross-section.

## 2.2 Test Matrix

The test plan (Table 1) was developed by the NASA Johnson Space Center Hypervelocity Impact Technology (HVIT) group in Houston, Texas. HVIT personnel constructed the targets, monitored the tests, measured and documented damage after completion of the tests. Aluminum 2017-T4 (density 2.796 g/cm<sup>3</sup>) and stainless steel 440C (density 7.667 g/cm<sup>3</sup>) spherical projectiles were used in the tests. All tests were performed between 6.8 km/s and 7.2 km/s, at an impact angle normal to the target (at 0° impact angle, measured from the target normal). The purpose of the tests was to find the projectile diameter at the failure threshold of the target, which was defined as either perforation or detached spall from the back side of the rear wall. A “pass” would therefore be no perforation or detached spall of the rear wall. This test objective necessitated impacts with projectiles on either side of the failure threshold or ballistic limit of the shield, i.e., to bracket the ballistic limit projectile diameter for a given impact velocity and angle. In some cases, two tests were performed for each test condition to evaluate repeatability (projectile velocity could vary slightly between these two tests, but projectile diameter and impact angle were kept constant). Near the ballistic limit of the shield, it was found that a particular test condition could result in either pass or fail due to small variations in impact velocity and/or the location of the projectile impact relative to the woven structure of the Nextel fabric.

## 3 TEST RESULTS

Results of the tests are provided in Table 1. The condition of the Nextel AF10 used in each test is indicated in Table 1, i.e., whether the Nextel has sizing (sized) or is heat-cleaned (HC). A comparison of the results is summarized in Table 2. As indicated, the results of the tests are similar between sized and heat-cleaned Nextel, particularly for aluminum projectiles. The tests with steel projectiles resulted in slightly better performance using the sized Nextel in the bumper than with heat-cleaned Nextel. However, even a small difference in performance could make a noticeable difference in MMOD risk assessment results, given the large change in orbital debris flux with size [4].

Table 1. Hypervelocity Test Data.

Test number	Nextel condition	Projectile type	Projectile diameter (cm)	Projectile mass (g)	Velocity (km/s)	Results: Pass/Fail of rear wall, damage to back of Rear Wall (RW)
HITF19298	Sized	Al	0.12	0.00255	7.06	Fail, RW: detached spall
HITF19302	Sized	Al	0.11	0.00200	7.20	Pass, RW: bump
HITF19306	Sized	Al	0.11	0.00203	6.93	Pass, RW: bump
HITF19260	HC	Al	0.11	0.00204	7.09	Pass, RW: flat
HITF19261	HC	Al	0.11	0.00201	7.04	Pass, RW: flat
HITF19327	Sized	Steel	0.07	0.00136	7.26	Fail, RW: detached spall
HITF19307	Sized	Steel	0.06	0.00090	7.06	Pass, RW: flat
HITF19326	Sized	Steel	0.06	0.00089	7.00	Pass, RW: bump
HITF19329	Sized	Steel	0.05	0.00049	7.09	Pass, RW: bump
HITF19278	HC	Steel	0.07	0.00136	6.94	Fail, RW: detached spall
HITF19300	HC	Steel	0.06	0.00087	6.95	Fail, RW: detached spall
HITF19301	HC	Steel	0.06	0.00087	6.92	Pass, RW: bump
HITF19309	HC	Steel	0.05	0.00049	7.08	Pass, RW: flat
HITF19310	HC	Steel	0.05	0.00049	7.03	Pass, RW: flat

Table 2. Summary of Results: Estimated projectile diameter on failure threshold of shield (for velocity between 6.8 km/s and 7.2 km/s, 0° impact angle).

Nextel Condition	Al critical diameter (cm)	Steel critical diameter (cm)	Comments
Sized	0.115	0.065	
Heat-Cleaned	0.115	0.06	Based on 1 pass, 1 fail with 0.06 cm



Figures 5 and 6 show the results of comparable tests for sized and heat-cleaned Nextel with aluminum projectiles. The rear wall damage (no-perforation or detached spall) is similar between the two Nextel conditions (sized and heat-cleaned). Because of its lower strength, the perforation hole sizes in the heat-cleaned Nextel bumper layers were expected to be larger than the equivalent tests on sized Nextel. However, this was not always the case. The perforation hole in the first Nextel layer with sizing is slightly larger than the perforation in the first layer of heat-cleaned Nextel (2.6 mm with sizing and 1.8 mm for the heat-cleaned Nextel), but the perforation hole in the second layer of sized Nextel is, as expected, smaller than the heat-cleaned Nextel (4.0 mm vs. 5.2 mm). This difference in Nextel hole sizes was also noted in the second series of tests with the same size aluminum projectile, although the difference was less pronounced.

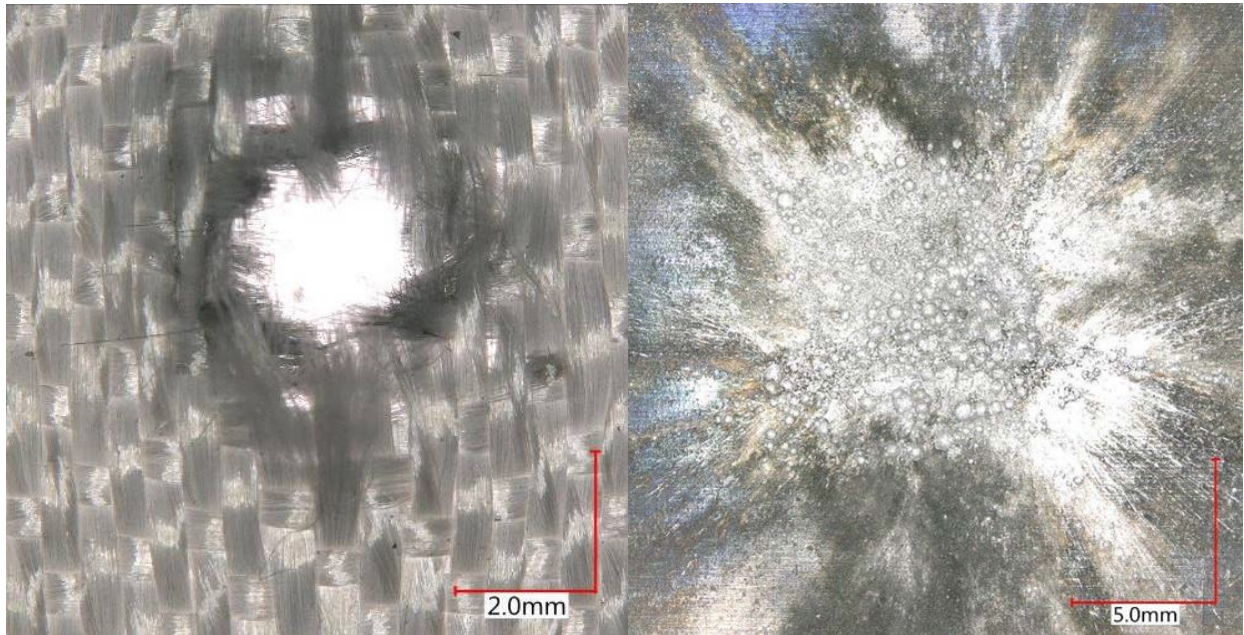


Fig. 5. Test number HITF19306, 1.1 mm Al projectile, 6.93 km/s, Nextel (sized) front layer perforation on left, rear wall craters on front of rear wall on right (bump on back of rear wall not shown).

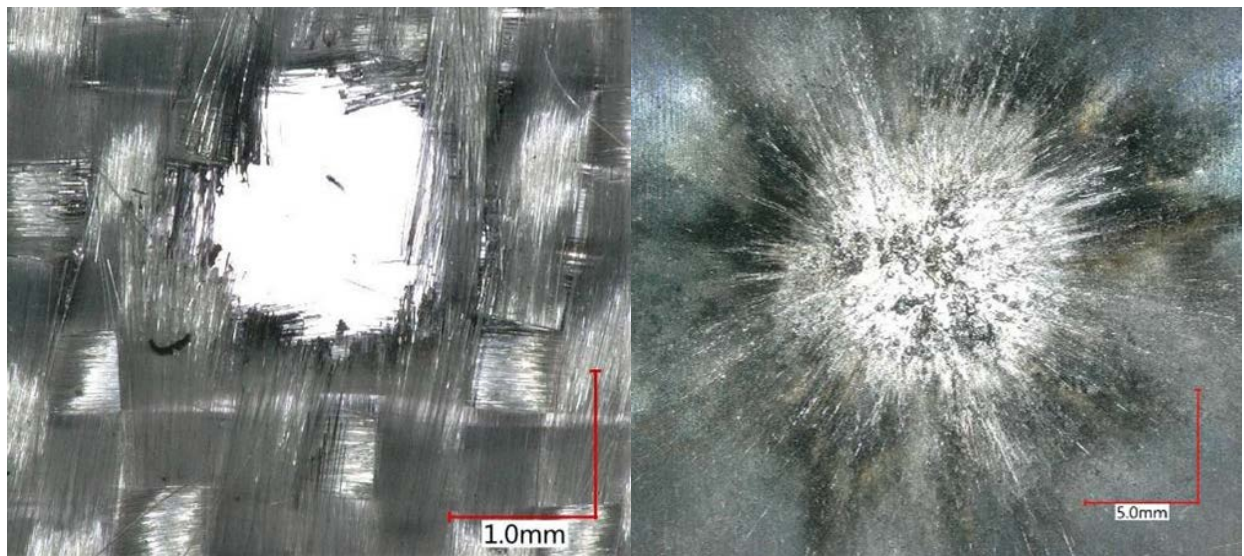


Fig. 6. Test number HITF19261, 1.1 mm Al projectile, 7.04 km/s, Nextel (heat-cleaned) front layer perforation on left, rear wall craters on front of rear wall on right (back of rear wall was flat, not shown).



Fig. 7 and Fig. 8 provide a similar comparison between Nextel conditions for steel projectiles. As described previously, there is slightly more damage to the rear wall with heat-cleaned Nextel bumper compared to the sized Nextel. For steel projectiles, the hole size in the sized Nextel first bumper layer and second layer are both smaller than the heat-cleaned Nextel hole size (1.3 mm vs. 2.0 mm in first layer of Nextel) and (2.1 mm vs. 4.4 mm in second layer), as expected due to the lower strength of the heat-cleaned Nextel.

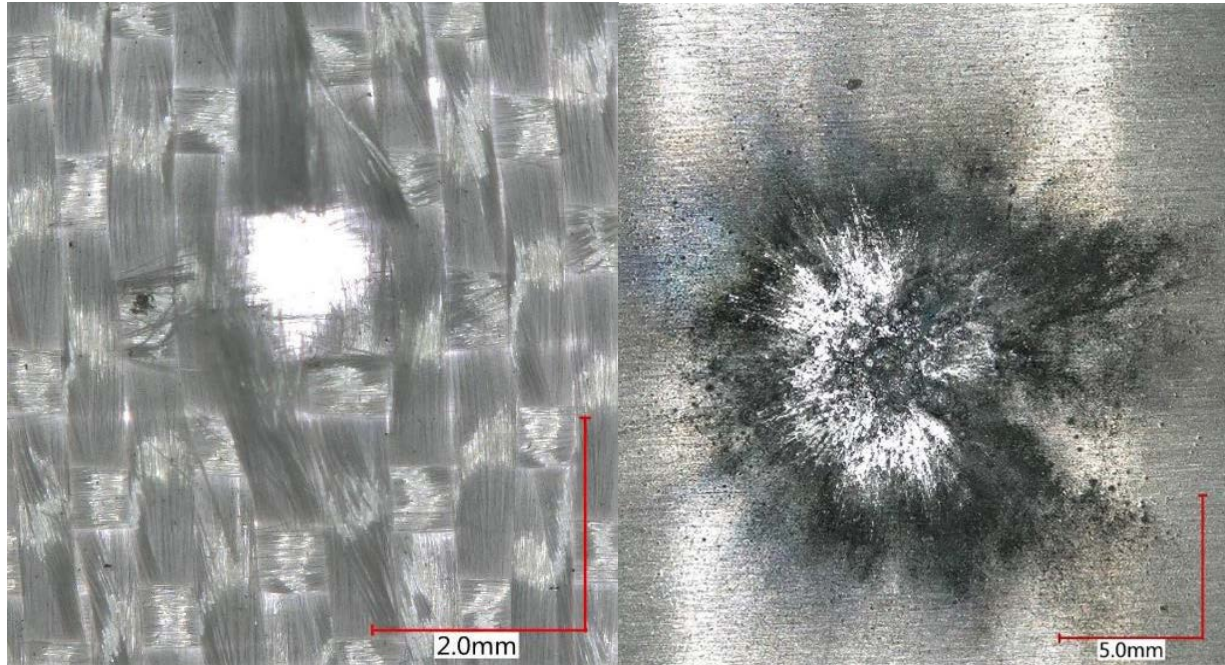


Fig. 7. Test number HITF19326, 0.6 mm steel projectile, 7.00 km/s, Nextel (sized) front layer perforation on left, rear wall craters on front of rear wall on right (bump on back of rear wall not shown).

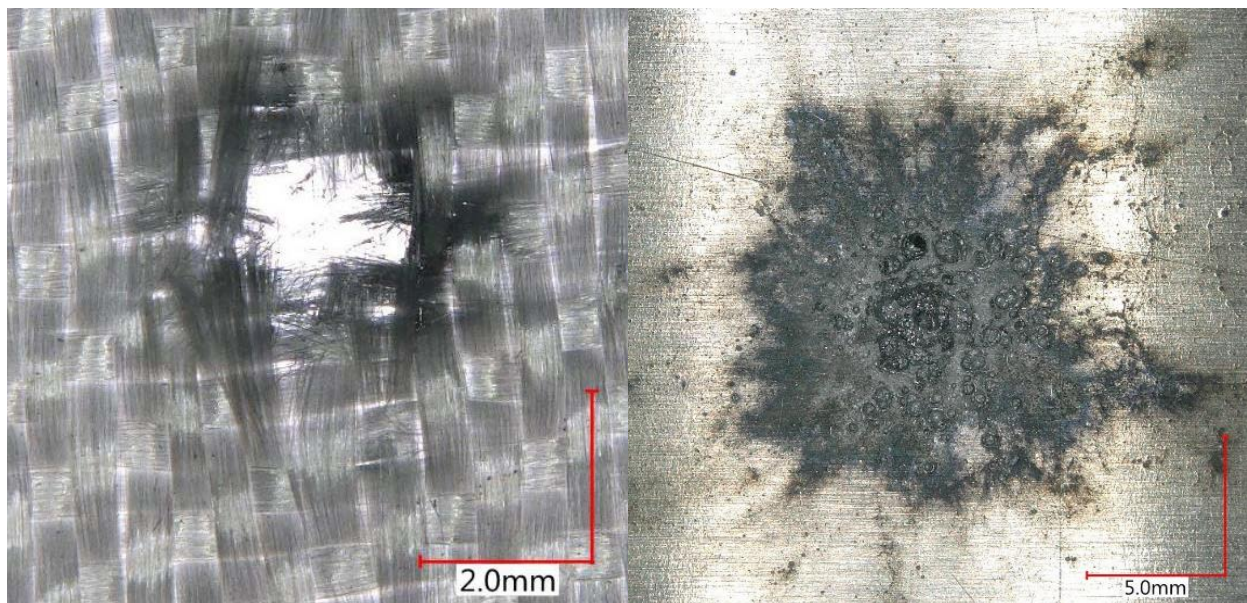


Fig. 8. Test number HITF19300, 0.6 mm steel projectile, 6.95 km/s, Nextel (heat-cleaned) front layer perforation on left, rear wall craters on right (4 mm diameter spall on back of rear wall not shown).

#### 4 BALLISTIC LIMIT EQUATIONS

Ballistic limit equations (BLEs) have been derived for the 2-layer Nextel shields evaluated in this work based on Whipple shield equations previously developed [5-8]. The BLEs are used to predict the critical projectile diameter,  $d_c$  (cm), on the threshold of shield failure, where failure is defined as rear wall perforation or detached spall. These equations were modified to reflect the fact that the areal density of the Nextel bumper is below the applicable value for these equations, namely the unmodified BLE [5] predicts an areal density of the critical projectile to bumper ratio of 0.08 at 7 km/s for normal impact ( $0^\circ$ ) of an aluminum projectile; i.e.,

$$m_p / m_b = d_c \rho_p / (t_b \rho_b) = 0.08 \text{ (for the unmodified BLE reported in [5, Eqs. 9-12])} \quad (1)$$

Where,

$m_p$  is the areal density of the projectile ( $\text{g/cm}^2$ ),

$m_b$  is the areal density of the bumper ( $\text{g/cm}^2$ ),

$d_c$  is the critical projectile diameter on threshold of shield failure (cm),

$\rho_p$  is the density of the projectile ( $\text{g/cm}^3$ ),

$t_b$  is the bumper thickness (cm), which for a Nextel bumper is  $t_b = m_b / 2.8 \text{ g/cm}^3$ ,

$\rho_b$  is the bumper density ( $\text{g/cm}^3$ ), namely the Nextel fiber density which is  $2.8 \text{ g/cm}^3$  (for Nextel 312 fiber).

The unmodified BLE is applicable for a 0.18 and higher ratio of areal density of the critical projectile to bumper, which implies the Nextel bumper is too thin for the particle size calculated by the unmodified equation. Based on the test results, the unmodified equation for the high-velocity regime was derated by a factor,  $f_H$ , which was slightly different for aluminum and steel projectiles, as follows:

High-Velocity: when  $V \geq V_H/(\cos\theta)$ ,

$$d_c = f_H k_H \rho_p^{-1/3} (V \cos\theta)^{-2/3} \rho_b^{-1/9} S^{1/3} t_w^{2/3} \sigma'_h{}^{1/3} \quad (2)$$

Where symbols not previously used are defined as follows:

$V_H = 7 \text{ km/s}$  for  $\rho_p < 6 \text{ g/cm}^3$ , and  $V_H = 9.1 \text{ km/s}$  for  $\rho_p \geq 6 \text{ g/cm}^3$ ,

$\theta$  is the impact angle (deg) measured from the target normal ( $\theta = 0^\circ$  is an impact normal to the target),

$\cos\theta$  is the cosine of the impact angle,

$f_H = 0.46$  for  $\rho_p < 6 \text{ g/cm}^3$  for both sized and heat-cleaned Nextel,

$f_H = 0.40$  for  $\rho_p \geq 6 \text{ g/cm}^3$  for sized Nextel, and  $f_H = 0.37$  for  $\rho_p \geq 6 \text{ g/cm}^3$  for heat-cleaned Nextel,

$k_H = 3.918$ ,

$V$  is impact velocity (km/s),

$S$  is shield standoff distance (cm),

$t_w$  is rear wall thickness (cm),

$\sigma'_h$  is the normalized yield stress (unitless)  $= (\sigma_w/70 \text{ ksi})$ , and  $\sigma_w = 36 \text{ ksi}$  for Al 6061-T6.

Note that the JSC HVIT performed numerous simulations, assessments and tests in the 2012-2013 time period to obtain the 9.1 km/s transition velocity for high-density projectiles [8].

Low-Velocity: when  $V \leq V_L/(\cos\theta)$ ,

$$d_c = \{ (t_w \sigma'_L{}^{0.5} + f_L m_b / \rho_b) / (0.6 (\cos\theta)^{5/3} \rho_p^{0.5} V^{2/3}) \}^{(19/18)} \quad (3)$$

Where,

$\sigma'_L$  is the normalized yield stress for low-velocity regime (unitless) =  $(\sigma_w/40 \text{ ksi})$ ,  $\sigma_w = 36 \text{ ksi}$  for Al 6061-T6,

$f_L$  is a factor to correct for the reduced strength of heat-cleaned Nextel relative to sized Nextel. Based on assumed strength reduction of around 50% for heat-cleaned Nextel,  $f_L = 0.7$  for heat-cleaned Nextel, and  $f_L = 1.0$  for sized Nextel.

**Intermediate-Velocity:** when  $V_L/(\cos\theta) < V < V_H/(\cos\theta)$ ,  $d_c$  is found by linear interpolation between high-velocity and low-velocity end points, or can be found as follows:

$$d_c = [k_h V_H^{-2/3} f_H \rho_p^{-1/3} \rho_b^{-1/9} S^{1/3} t_w^{2/3} \sigma'_h{}^{1/3}] \\ [V - V_L(\cos\theta)^{-1}] / [V_H(\cos\theta)^{-1} - V_L(\cos\theta)^{-1}] \\ + \{ (t_w \sigma'_L{}^{0.5} + f_L m_b / \rho_b) / (0.6 V_L^{2/3} \rho_p^{0.5} (\cos\theta)) \}^{(18/19)} \\ [V_H(\cos\theta)^{-1} - V] / [V_H(\cos\theta)^{-1} - V_L(\cos\theta)^{-1}] \quad (4)$$

Because Nextel bumper fragments have little damage potential for the rear wall in normal and oblique impacts, there is no impact angle cutoff for highly oblique impacts (above  $65^\circ$ ).

Figure 9 compares hypervelocity impact data for sized Nextel with the predicted ballistic limits based on Eqs. 2-4 (normal impact angle with aluminum and steel projectiles). Figure 10 provides a similar comparison for heat-cleaned (HC) Nextel. Figure 11 compares sized and heat-cleaned ballistic limits at normal ( $0^\circ$ ) impact angle for aluminum and steel projectiles, indicating there is not much difference in the BLEs for these two different conditions (sized and heat-cleaned). Figure 12 shows the predicted ballistic limit curves for sized Nextel at three impact angles:  $0^\circ$ ,  $45^\circ$ , and  $60^\circ$ .

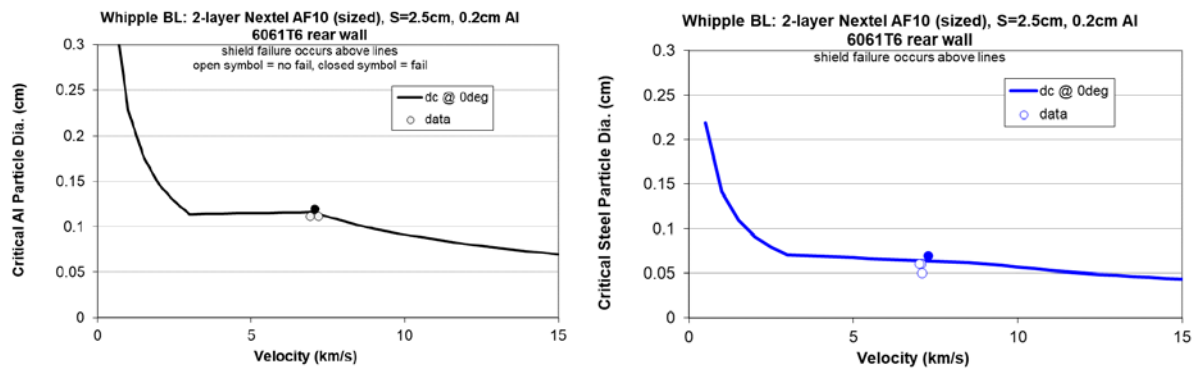


Fig. 9. Ballistic limits (BLs) for sized Nextel shields compared to test data at normal impact angle (Al projectiles on left, steel on right).

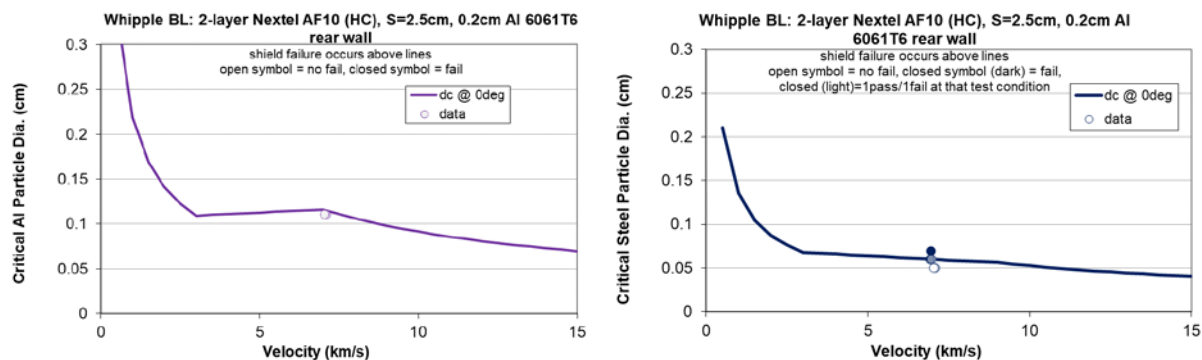


Fig. 10. BLs for HC Nextel shields compared to test data at normal impact angle (Al projectiles on left, steel on right).



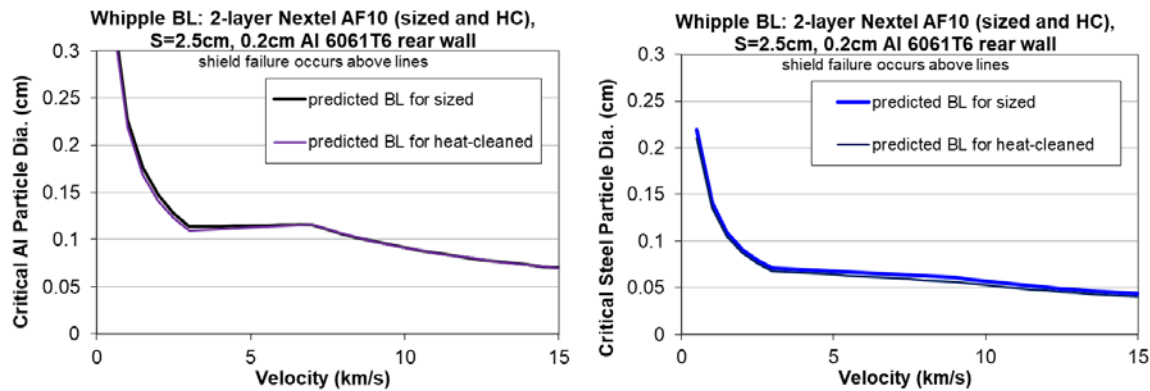


Fig. 11. Comparison between sized and heat-cleaned BLs at normal impact angle (Al projectiles on left, steel on right).

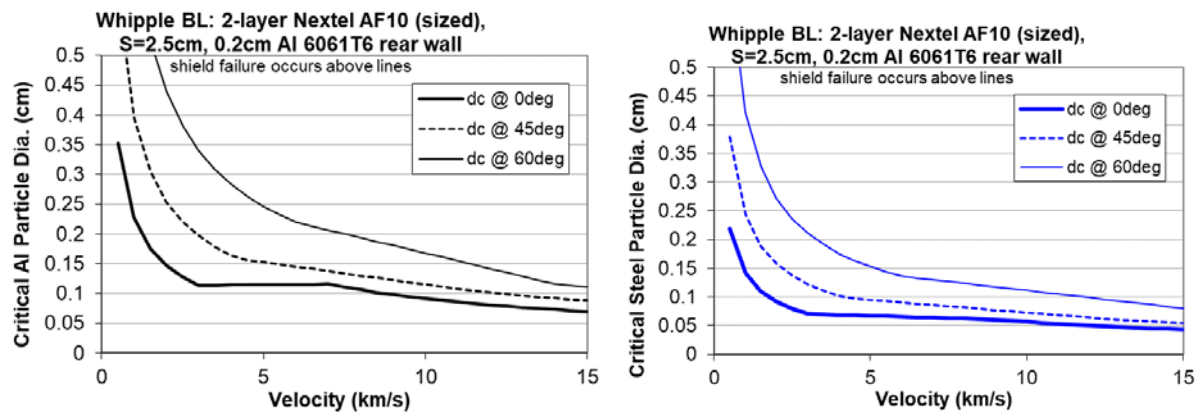


Fig. 12. BLs for 0°, 45°, and 60° impact angle, for sized Nextel shields (aluminum projectiles on left, steel on right).

## 5 CONCLUSIONS

This paper described the results of hypervelocity impact tests evaluating the difference between sized and heat-cleaned Nextel 312 style AF10 fabric used as a first bumper in MMOD shielding. The heat-cleaned Nextel is approximately 17% lighter (on mass per unit area basis) than the sized Nextel. No appreciable difference in ballistic performance was determined for aluminum projectile impacts between the two Nextel conditions (sized and heat-cleaned). A minor decrease in the heat-cleaned shield performance was observed compared with sized Nextel at normal impact of steel spherical projectiles at 7 km/s. Ballistic limit equations were provided for the tested shield, with adjustments made to fit test data. Additional testing is underway on a different shield type (Fig. 13), and at oblique impact angles and at different impact speeds.

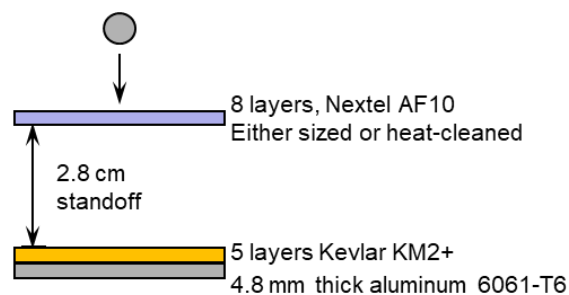


Fig. 13. Alternative shield type using Nextel bumper and Kevlar/Aluminum rear wall.

**REFERENCES**

1. E.L. Christiansen, K. Nagy, D.M. Lear, T.G. Prior, Space Station MMOD Shielding, IAC-06-B6.3.05, 57th International Astronautical Congress, <https://ntrs.nasa.gov/archive/nasa/casi.ntrs.nasa.gov/20060026214.pdf>, 2006.
2. 3M™ Nextel™ Ceramic Fibers and Textiles: Technical Reference Guide, available at: <https://multimedia.3m.com/mws/media/1327055O/3m-nextel-technical-reference-guide.pdf>.
3. JSC Partnership Gateway, Hypervelocity Impact and Orbital Debris, <https://www.nasa.gov/centers/johnson/partnerships/erc/hypervelocity-impact-orbital-debris>
4. E.G. Stansbery, et al., NASA Orbital Debris Engineering Model ORDEM 3.0 – Verification and Validation, NASA TP-2015-218592, 2015.
5. E.L. Christiansen, Design and Performance Equations for Advanced Meteoroid and Debris Shields, International Journal of Impact Engineering, Vol.14, pp.145-156 (1993), Proceedings of the 1992 HVIS, November 1992.
6. E.L. Christiansen, Meteoroid/Debris Shielding, NASA Technical Publication, NASA/TP-2003-210788, 2003.
7. E.L. Christiansen, J. Arnold, A. Davis, J. Hyde, D. Lear, J.-C. Liou, F. Lyons, T. Prior, M. Ratliff, S. Ryan, F. Giovane, R. Corsaro, G. Studor, Handbook for Designing MMOD Protection, NASA TM-2009-214785, 2009.
8. M. Squire, E.L. Christiansen, et al., NASA/TM-2014-218268, Volume I & II, Micrometeoroid and Orbital Debris (MMOD) Design and Analysis Improvements, NASA Engineering and Safety Center Report NESC-RP-12-00780, 2014.